Available online at www.sciencedirect.com
ScienceDirect
Journal of Process Control 17 (2007) 439–451
JOURNAL OF PROCESS CONTROL
www.elsevier.com/locate/jprocont

Fault-tolerant control of a polyethylene reactor

Adiwinata Gani [a], Prashant Mhaskar [b], Panagiotis D. Christofides [a,*]

[a] Department of Chemical and Biomolecular Engineering, University of California, Los Angeles, CA 90095, United States
[b] Department of Chemical Engineering, McMaster University, Hamilton, ON, Canada L8S4L7

Received 15 November 2005; accepted 14 April 2006

Abstract

This work focuses on fault-tolerant control of a gas phase polyethylene reactor. Initially, a family of candidate control configurations, characterized by different manipulated inputs, is identified. For each control configuration, a bounded nonlinear feedback controller, that enforces asymptotic closed-loop stability in the presence of constraints, is designed, and the constrained stability region associated with it is explicitly characterized using Lyapunov-based tools. Next, a fault-detection filter is designed to detect the occurrence of a fault in the control actuator by observing the deviation of the process states from the expected closed-loop behavior. A switching policy is then derived, on the basis of the stability regions, to orchestrate the activation/deactivation of the constituent control configurations in a way that guarantees closed-loop stability in the event of control system faults. Closed-loop system simulations demonstrate the effectiveness of the fault-tolerant control strategy.

Keywords: Fault-tolerant control; Fault-detection; Input constraints; Stability region; Lyapunov-based control; Polyethylene reactor

1. Introduction

Increasingly faced with the requirements of safety, reliability, and profitability, chemical process operation is relying extensively on highly automated process control systems. Automation, however, tends to increase vulnerability of the process to faults (for example, defects/malfunctions in process equipment, sensors and actuators, faults in the controllers or in the control loops) potentially causing a host of economic, environmental, and safety problems that can seriously degrade the operating efficiency of the process. Problems due to faults may include physical damage to the process equipment, increase in the wasteful use of raw material and energy resources, increase in the downtime for process operation resulting in significant production losses, and jeopardizing personnel and environmental safety. These considerations provide a strong motivation for the development of methods for the design of advanced fault-tolerant control systems that ensure an efficient and timely response to enhance fault recovery and prevent faults from propagating or developing into total faults.

Fault-tolerant control has been an active area of research for the past 10 years, and has motivated many research studies in this area within the context of aerospace engineering (see, for example, [37,3,47]). The whole notion of fault-tolerant control is based on the underlying assumption of the availability of more control configurations than required. Under this assumption, the reliable control approach (see, for example, [45,41]) dictates use of all the control loops at the same time so that fault in one control loop does not lead to the failure of the entire control structure. The use of only as many control loops as are required at a time, is often motivated by economic considerations (to save on unnecessary control action), and in this case, fault-tolerant control can be achieved through control-loop reconfiguration. Recently, fault-tolerant control has gained increased attention within process control; however, the available results have been based on the assumption of a linear process description [23,43,2,38].

* Corresponding author. Tel.: +1 310 794 1015; fax: +1 310 206 4107.
E-mail address: pdc@seas.ucla.edu (P.D. Christofides).

0959-1524/$ - see front matter © 2006 Elsevier Ltd. All rights reserved.
doi:10.1016/j.jprocont.2006.04.002

One of the prerequisites in implementing fault-tolerant control is the ability to detect and isolate the occurrence of faults. Existing results on the design of fault-detection filters include those that use past plant-data and those that use fundamental process models for the purpose of fault-detection filter design. Statistical and pattern recognition techniques for data analysis and interpretation (for example, [25,39,36,12,35,11,7,42,1,46]) use past plant-data to construct indicators that identify deviations from normal operation to detect faults. The problem of using fundamental process models for the purpose of detecting faults has been studied extensively in the context of linear systems [27,19,20,9,29] and more recently some existential results in the context of nonlinear systems have been derived [40,10].

A switch to fall-back control configuration (upon detection of a fault in a control configuration) results in an overall process that exhibits intervals of piecewise continuous behavior interspersed by discrete transitions. A hybrid systems framework therefore provides a natural setting for the analysis and design of fault-tolerant control structures. However, at this stage, despite the large and growing body of research work on a diverse array of hybrid system problems (for example, [22,21,8,15,31,5]), the use of a hybrid system framework for the study of fault-tolerant control problems has received limited attention. In [16], a hybrid systems approach to fault-tolerant control was employed where upon occurrence of a fault, stability region-based reconfiguration is done to achieve fault-tolerant control. In [34], the problem of implementing integrated fault-detection and fault-tolerant control (FDFTC) was addressed under state and output feedback control and in [33], performance and robustness considerations were incorporated in the fault-tolerant control structure.

Industrial processes stand to gain from an application of fault-tolerant control structures that prevent loss of product (due, for example, to limit cycles) and possible loss of equipment (due, for example, to unacceptably high temperatures) in the event of a fault in the control configuration, while accounting explicitly for the complex process characteristics manifested in the form of nonlinearities, constraints and uncertainty. Motivated by these considerations, this work focuses on fault-tolerant control of a gas phase polyethylene reactor modeled by seven nonlinear ordinary differential equations (ODEs). Polyethylene is the most popular of all synthetic commodity polymers, with current worldwide production of more than 40 billion tonnes per year. Large proportion of this polyethylene is produced in gas phase reactors using Ziegler-Natta catalysts. In a gas phase polyethylene reactor, the temperature in the reaction zone is kept above the dew point of the reactant and below the melting point of the polymer to prevent melting and consequent agglomeration of the product particles. Most commercial gas phase fluidized bed polyethylene reactors are operated in a relatively narrow temperature range between 75 °C and 110 °C [44]. It has been demonstrated [4,28,24] that without feedback temperature control (or in the event of failure in the control configuration), industrial gas phase polyethylene reactors are prone to unstable steady-states, limit cycles, and excursions toward unacceptable high temperature steady-states which can lead to loss of product as well as damage the equipment.

To develop a fault-tolerant control system for the gas phase polyethylene reactor, we initially describe the process evolution on the basis of a detailed model and identify a family of candidate control configurations. For each control configuration, a bounded nonlinear feedback controller, that enforces asymptotic closed-loop stability in the presence of constraints, is designed, and the constrained stability region associated with it is explicitly characterized using Lyapunov-based tools. Next, a fault-detection filter is designed to detect the occurrence of a fault in the control actuator by observing the deviation of the process states from the expected closed-loop behavior. A switching policy is then derived, on the basis of the stability regions, to orchestrate the activation/deactivation of the constituent control configurations in a way that guarantees closed-loop stability in the event of control system faults. Closed-loop system simulations demonstrate the effectiveness of the fault-tolerant control strategy as well as investigate an application in the presence of measurement noise.

2. Process description and modeling

Fig. 1 shows a schematic of an industrial gas phase polyethylene reactor system. The feed to the reactor consists of ethylene, comonomer, hydrogen, inerts, and catalyst. A stream of unreacted gases flows from the top of the reactor and is cooled by passing through a heat exchanger in counter-current flow with cooling water. Cooling rates in the heat exchanger are adjusted by instantaneously blending cold and warm water streams while maintaining a constant total cooling water flowrate through the heat exchanger.

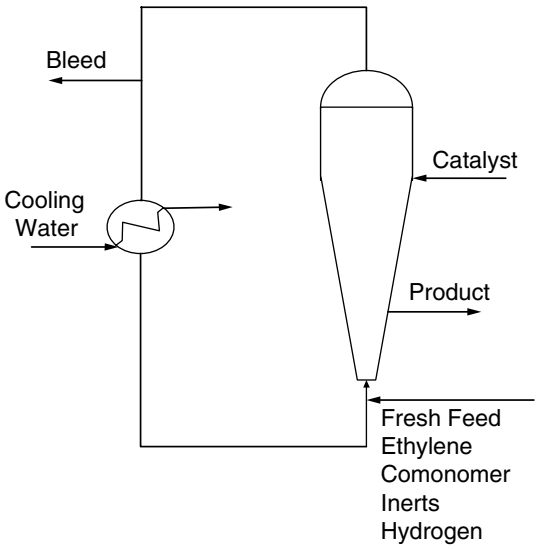

Fig. 1. Industrial gas phase polyethylene reactor system.

Mass balance on hydrogen and comonomer have not been considered in this study because hydrogen and comonomer have only mild effects on the reactor dynamics [28]. A mathematical model for this reactor has the form [6]:

$$\begin{aligned}
\frac{\mathrm{d}[In]}{\mathrm{d}t} &= \frac{F_{In} - \frac{[In]}{[M_1]+[In]} b_t}{V_g} \\
\frac{\mathrm{d}[M_1]}{\mathrm{d}t} &= \frac{F_{M_1} - \frac{[M_1]}{[M_1]+[In]} b_t - R_{M1}}{V_g} \\
\frac{\mathrm{d}Y_1}{\mathrm{d}t} &= F_c a_c - k_{d_1} Y_1 - \frac{R_{M1} M_{W_1} Y_1}{B_w} \\
\frac{\mathrm{d}Y_2}{\mathrm{d}t} &= F_c a_c - k_{d_2} Y_2 - \frac{R_{M1} M_{W_1} Y_2}{B_w} \\
\frac{\mathrm{d}T}{\mathrm{d}t} &= \frac{H_f + H_{g1} - H_{g0} - H_r - H_{pol}}{M_r C_{pr} + B_w C_{ppol}} \\
\frac{\mathrm{d}T_{w_1}}{\mathrm{d}t} &= \frac{F_w}{M_w}(T_{wi} - T_{w_1}) - \frac{UA}{M_w C_{pw}}(T_{w_1} - T_{g_1}) \\
\frac{\mathrm{d}T_{g_1}}{\mathrm{d}t} &= \frac{F_g}{M_g}(T - T_{g_1}) + \frac{UA}{M_g C_{pg}}(T_{w_1} - T_{g_1})
\end{aligned} \tag{2.1}$$

where

$$\begin{aligned}
b_t &= V_p C_v \sqrt{([M_1] + [In]) \cdot RR \cdot T - P_v} \\
R_{M1} &= [M_1] \cdot k_{p0} \cdot \exp\left[\frac{-E_a}{R}\left(\frac{1}{T} - \frac{1}{T_f}\right)\right] \cdot (Y_1 + Y_2) \\
C_{pg} &= \frac{[M_1]}{[M_1] + [In]} C_{pm1} + \frac{[In]}{[M_1] + [In]} C_{pIn} \\
H_f &= F_{M_1} C_{pm1}(T_{\text{feed}} - T_f) + F_{In} C_{pIn}(T_{\text{feed}} - T_f) \\
H_{g1} &= F_g(T_{g_1} - T_f) C_{pg} \\
H_{g0} &= (F_g + b_t)(T - T_f) C_{pg} \\
H_r &= H_{\text{reac}} M_{W_1} R_{M1} \\
H_{pol} &= C_{ppol}(T - T_f) R_{M1} M_{W_1}
\end{aligned} \tag{2.2}$$

Table 1 includes the definition of all the variables used in Eqs. (2.1) and (2.2). The values of the process parameters are listed in Table 2. Under these operating conditions, the open-loop system behaves in an oscillatory fashion (i.e., the system possesses an open-loop unstable steady-state surrounded by a limit cycle).

The control objective is to stabilize the reactor. To accomplish this objective we consider the following manipulated input candidates:

(1) Feed temperature, $u_1 = \frac{F_{M_1} C_{pm1} + F_{In} C_{pIn}}{M_r C_{pr} + B_w C_{ppol}}(T_{\text{feed}} - T^s_{\text{feed}})$, subject to the constraint $|u_1| \leqslant u^1_{\max} = \frac{F_{M_1} C_{pm1} + F_{In} C_{pIn}}{M_r C_{pr} + B_w C_{ppol}}(20)\,\frac{K}{s}$.

Table 1
Process variables

a_c	Active site concentration of catalyst
b_t	Overhead gas bleed
B_w	Mass of polymer in the fluidized bed
C_{pm1}	Specific heat capacity of ethylene
C_v	Vent flow coefficient
C_{pw}, C_{pIn}, C_{ppol}	Specific heat capacity of water, inert gas and polymer
E_a	Activation energy
F_c, F_g	Flow rate of catalyst and recycle gas
F_{In}, F_{M_1}, F_w	Flow rate of inert, ethylene and cooling water
H_f, H_{g0}	Enthalpy of fresh feed stream, total gas outflow stream from reactor
H_{g1}	Enthalpy of cooled recycle gas stream to reactor
H_{pol}	Enthalpy of polymer
H_r	Heat liberated by polymerization reaction
H_{reac}	Heat of reaction
$[In]$	Molar concentration of inerts in the gas phase
k_{d_1}, k_{d_2}	Deactivation rate constant for catalyst site 1, 2
k_{p0}	Pre-exponential factor for polymer propagation rate
$[M_1]$	Molar concentration of ethylene in the gas phase
M_g	Mass holdup of gas stream in heat exchanger
$M_r C_{pr}$	Product of mass and heat capacity of reactor walls
M_w	Mass holdup of cooling water in heat exchanger
M_{W_1}	Molecular weight of monomer
P_v	Pressure downstream of bleed vent
R, RR	Ideal gas constant, unit of $\frac{\text{J}}{\text{mol K}}$, $\frac{\text{m}^3\,\text{atm}}{\text{mol K}}$
T, T_f, T_{feed}	Reactor, reference, feed temperature
T_{g_1}, T_{w_1}	Temperature of recycle gas, cooling water stream from exchanger
T_{wi}	Inlet cooling water temperature to heat exchanger
UA	Product of heat exchanger coefficient with area
V_g	Volume of gas phase in the reactor
V_p	Bleed stream valve position
Y_1, Y_2	Moles of active site type 1, 2

Table 2
Parameter values and units

V_g	500	m^3
V_p	0.5	
P_v	17	atm
B_w	7×10^4	kg
k_{p0}	85×10^{-3}	$\frac{\text{m}^3}{\text{mol s}}$
E_a	(9000)(4.1868)	$\frac{\text{J}}{\text{mol}}$
C_{pm1}	(11)(4.1868)	$\frac{\text{J}}{\text{mol K}}$
C_v	7.5	$\text{atm}^{-0.5}\,\frac{\text{mol}}{\text{s}}$
C_{pw}, C_{pIn}	$(10^3)(4.1868)$, (6.9)(4.1868)	$\frac{\text{J}}{\text{kg K}}$
C_{ppol}	$(0.85 \times 10^3)(4.1868)$	$\frac{\text{J}}{\text{kg K}}$
k_{d_1}	0.0001	s^{-1}
k_{d_2}	0.0001	s^{-1}
M_{W_1}	28.05×10^{-3}	$\frac{\text{kg}}{\text{mol}}$
M_w	3.314×10^4	kg
M_g	6060.5	mol
$M_r C_{pr}$	$(1.4 \times 10^7)(4.1868)$	$\frac{\text{J}}{\text{K}}$
H_{reac}	$(-894 \times 10^3)(4.1868)$	$\frac{\text{J}}{\text{kg}}$
UA	$(1.14 \times 10^6)(4.1868)$	$\frac{\text{J}}{\text{K s}}$
F_{In}, F_{M_1}, F_g	5, 190, 8500	$\frac{\text{mol}}{\text{s}}$
F_w	$(3.11 \times 10^5)(18 \times 10^{-3})$	$\frac{\text{kg}}{\text{s}}$
F^s_c	$\frac{5.8}{3600}$	$\frac{\text{kg}}{\text{s}}$
T_f, T^s_{feed}, T_{wi}	360, 293, 289.56	K
RR	8.20575×10^{-5}	$\frac{\text{m}^3\,\text{atm}}{\text{mol K}}$
R	8.314	$\frac{\text{J}}{\text{mol K}}$
a_c	0.548	$\frac{\text{mol}}{\text{kg}}$
$u^{\max}_1$, $u^{\max}_2$	5.78×10^{-4}, 3.04×10^{-4}	$\frac{\text{K}}{\text{s}}$, $\frac{\text{mol}}{\text{s}}$
$[In]_s$	439.68	$\frac{\text{mol}}{\text{m}^3}$
$[M_1]_s$	326.72	$\frac{\text{mol}}{\text{m}^3}$
Y_{1_s}, Y_{2_s}	3.835, 3.835	mol
T_s, $T_{w_{1_s}}$, $T_{g_{1_s}}$	356.21, 290.37, 294.36	K

(2) Catalyst flowrate, $u_2 = (F_c - F_c^s)a_c$, subject to the constraint $|u_2| \leqslant u_{\max}^2 = \left(\frac{2}{3600}\right)a_c \ \frac{\text{mol}}{\text{s}}$.

Each of the above manipulated inputs represents a unique control configuration (or control loop) that, by itself, can stabilize the reactor. The first control configuration, with feed temperature (T_{feed}) as the manipulated input, will be considered as the primary configuration. In the event of some faults in this configuration, however, the plant supervisor, will have to activate the fall-back configuration in order to maintain closed-loop stability. The question which we address in the next section, is how the supervisor determines, from observing the evolution of the process, that a fault has occurred in the control configuration and whether or not the fall-back control configuration will be able to stabilize the reactor if the primary control configuration fails.

3. Fault-tolerant control

Having identified the candidate control configurations that can be used, we outline in this section the main steps involved in the fault-tolerant control system design procedure. These include: (a) the synthesis of a stabilizing feedback controller for each control configuration, (b) the explicit characterization of the constrained stability region associated with each configuration, (c) the design of a fault-detection filter, and (d) the design of a switching law that orchestrates the re-configuration of control system in a way that guarantees closed-loop stability in the event of faults in the active control configuration.

To present our results in a compact form, we write the model of Eq. (2.1) in a deviation (from the operating unstable steady-state) variable form, by defining $x = [x_1\ x_2\ x_3\ x_4\ x_5\ x_6\ x_7]^{\mathrm{T}}$ where $x_1 = In - In_s$, $x_2 = M_1 - M_{1_s}$, $x_3 = Y_1 - Y_{1_s}$, $x_4 = Y_2 - Y_{2_s}$, $x_5 = T - T_s$, $x_6 = T_{w_1} - T_{w_{1s}}$, $x_7 = T_{g_1} - T_{g_{1_s}}$, and obtain a continuous-time nonlinear system with the following state-space description:

$$\begin{aligned} &\dot{x}(t) = f_{k(t)}(x(t)) + g_{k(t)}(x(t))u_{k(t)} \\ &|u_{k(t)}| \leqslant u_k^{\max} \\ &k(t) \in K = \{1, 2\} \end{aligned} \tag{3.3}$$

where $x(t) \in \mathbb{R}^7$ denotes the vector of process state variables and $u_k(t) \in [-u_k^{\max}, u_k^{\max}] \subset \mathbb{R}$ denotes the constrained manipulated input associated with the kth control configuration. $k(t)$, which takes values in the finite index set K, represents a discrete state that indexes the vector fields $f_k(\cdot)$, $g_k(\cdot)$ as well as the manipulated input $u_k(\cdot)$. The explicit form of the vector fields $f_{k(t)}(x(t))$ and $g_{k(t)}(x(t))$ can be obtained by comparing Eqs. (2.1) and (3.3) and is omitted for brevity. For each value that k assumes in K, the process is controlled via a different manipulated input which defines a given control configuration. Switching between the two available control configurations is controlled by a higher-level supervisor that monitors the process and orchestrates, accordingly, the transition between the different control configurations in the event of control system fault. This in turn determines the temporal evolution of the discrete state, $k(t)$. The supervisor ensures that only one control configuration is active at any given time, and allows only a finite number of switches over any finite interval of time. The control objective is to stabilize the process of Eq. (3.3) in the presence of actuator constraints and faults in the control system. The basic problem is how to detect the occurrence of a fault and coordinate switching between the different control configurations (or manipulated inputs) in a way that respects actuator constraints and guarantees closed-loop stability in the event of faults. To simplify the presentation of our results, we will focus only on the state feedback problem where measurements of all process states are available for all times.

3.1. Constrained feedback controller synthesis

In this step, we synthesize, for each control configuration, a feedback controller that enforces asymptotic closed-loop stability in the presence of actuator constraints. This task is carried out on the basis of the process input/output dynamics. While our control objective is to achieve full state stabilization, process outputs are introduced only to facilitate transforming the system of Eq. (2.1) into a form more suitable for explicit controller synthesis.

1. For the primary control configuration with $u_1 = \frac{F_{M_1}C_{pm1} + F_{In}C_{pln}}{M_rC_{pr} + B_wC_{ppol}}(T_{\text{feed}} - T_{\text{feed}}^s)$, we consider the output $y_1 = T - T_s$. This choice yields a relative degree of $r_1 = 1$ with respect to u_1. The input/output dynamics can be then expressed in terms of the time-derivative of the variable: $e_1 = T - T_s$.
2. For the fall-back control configuration with $u_2 = (F_c - F_c^s)a_c$, we choose the output $y_2 = T - T_s$ which yields a relative degree of $r_2 = 2$ and the corresponding variables for describing the input/output dynamics take the form: $e_2^1 = T - T_s$, $e_2^2 = \frac{H_f + H_{g1} - H_{g0} - H_r - H_{pol}}{M_rC_{pr} + B_wC_{ppol}}$. In particular, for the fall-back control configuration, the system describing the input/output dynamics has the following form:

$$\dot{e}_2 = A_2e_2 + l_2(e_2) + b_2\alpha_2u_2 := \bar{f}_2(e_2) + \bar{g}_2(e_2)u_2 \tag{3.4}$$

where

$$A_2 = \begin{bmatrix} 0 & 1 \\ 0 & 0 \end{bmatrix}, \quad b_2 = \begin{bmatrix} 0 \\ 1 \end{bmatrix}, \quad e_2 = \begin{bmatrix} e_2^1 \\ e_2^2 \end{bmatrix},$$

$$l_2(\cdot) = L_{f_2}^2h_2(x), \quad \alpha_2(\cdot) = L_{g_2}L_{f_2}h_2(x)$$

$h_2(x) = y_2$ is the output associated with the fall-back control configuration (the explicit form of the functions $f_2(\cdot)$ and $g_2(\cdot)$ is omitted for brevity).

The inverse dynamics, for both the first and second control configurations, have the following form:

$$\begin{aligned}\dot{\eta}_1 &= \Psi_{1,k}(e,\eta)\\ &\vdots\\ \dot{\eta}_{7-r_k} &= \Psi_{7-r_k,k}(e,\eta)\end{aligned} \tag{3.5}$$

where $k = 1, 2$ and $\Psi_{1,k} \cdots \Psi_{7-r_k,k}$ are nonlinear functions of their arguments describing the evolution of the inverse dynamics of the kth mode.

Using a quadratic Lyapunov function of the form $V_k = e_k^{\mathrm{T}} P_k e_k$, where P_k is a positive-definite symmetric matrix that satisfies the Riccati inequality $A_k^{\mathrm{T}} P_k + P_k A_k - P_k b_k b_k^{\mathrm{T}} P_k < 0$, we synthesize, for each control-loop, a bounded nonlinear feedback control law (see [26,13,14]) of the form:

$$u_k = -r(x, u_k^{\max}) L_{\bar{g}_k} V_k \tag{3.6}$$

where

$$r(x, u_k^{\max}) = \frac{L^*_{\bar{f}_k} V_k + \sqrt{\left(L^*_{\bar{f}_k} V_k\right)^2 + \left(u_k^{\max} |L_{\bar{g}_k} V_k|\right)^4}}{\left(|L_{\bar{g}_k} V_k|\right)^2 \left[1 + \sqrt{1 + \left(u_k^{\max} |L_{\bar{g}_k} V_k|\right)^2}\right]} \tag{3.7}$$

and $L^*_{\bar{f}_k} V_k = L_{\bar{f}_k} V_k + \rho |e_k|^2$, $\rho > 0$. The scalar function $r(\cdot)$ in Eqs. (3.6) and (3.7) can be considered as a nonlinear controller gain. It can be shown that each control configuration asymptotically stabilizes the e states in each mode. This result, together with the property of the η states to be input-to-state stable, can be used to show, via a small gain argument, asymptotic stability for each control configuration (verified through simulation and analysis of the system of Eq. (3.7) with $e_k = 0$ for both $k = 1$ and $k = 2$). This controller gain, which depends on both the size of actuator constraints, $u_k^{\max}$, and the particular configuration used is shaped in a way that guarantees constraint satisfaction and asymptotic closed-loop stability within a well-characterized region in the state-space. The characterization of this region is discussed in the next step.

3.2. Characterization of constrained stability regions

Given that actuator constraints place fundamental limitations on the initial conditions that can be stabilized, it is important for the control system designer to explicitly characterize these limitations by identifying, for each control configuration, the set of admissible initial conditions starting from where the constrained closed-loop system is asymptotically stable. As discussed in step (d) below, this characterization is necessary for the design of an appropriate switching policy that ensures the fault-tolerance of the control system. The control law designed in step (a) provides such a characterization. Specifically, using a Lyapunov argument, one can show that the set

$$\Theta(u_k^{\max}) = \{x \in \mathbb{R}^7 : L^*_{\bar{f}_k} V_k \leqslant u_k^{\max} |L_{\bar{g}_k} V_k|\} \tag{3.8}$$

describes a region in the state space where the control action satisfies the constraints and the time-derivative of the corresponding Lyapunov function is negative-definite along the trajectories of the closed-loop system. Note that the size of this set depends, as expected, on the magnitude of the constraints. In particular, the set becomes smaller as the constraints become tighter (smaller $u_k^{\max}$). For a given control configuration, one can use the above inequality to estimate the stability region associated with this configuration. This can be done by constructing the largest invariant subset of Θ, which we denote by $\Omega(u_k^{\max})$. Confining the initial conditions within the set $\Omega(u_k^{\max})$ ensures that the closed-loop trajectory stays within the region defined by $\Theta(u_k^{\max})$, and thereby V_k continues to decay monotonically, for all times that the kth control configuration is active (see [13] for further discussion on this issue).

An estimate of the region of constrained closed-loop stability for the full system is obtained by defining a composite Lyapunov function of the form $V_{c_k} = V_k + V_{\eta_k}$, where $V_{\eta_k} = \eta^{\mathrm{T}} P_{\eta_k} \eta$ and P_{η_k} is a positive definite matrix and choosing a level set of V_{c_k}, Ω_{c_k}, for which $\dot{V}_{c_k} < 0$ for all x in Ω_{c_k}.

Remark 1. Note that the composite Lyapunov functions, V_{c_k}, used in implementing the switching rules, are in general different from the Lyapunov functions V_k used in designing the controllers. Owing to the ISS property of the η_k-subsystem of each mode, only a Lyapunov function for the e_k subsystem, namely V_k, is needed and used to design a controller that stabilizes the full $e_k - \eta_k$ interconnection for each mode. However, when implementing the switching rules (constructing the Ω_{c_k}), we need to track the evolution of x (and hence the evolution of both e_k and η_k). Therefore, the Lyapunov functions used in verifying the switching conditions at any given time, V_{c_k}, are based on x. From the asymptotic stability of each mode, the existence of these Lyapunov functions is guaranteed by converse Lyapunov theorems. Note also that the above controller design is only one example of a controller design that allows for an explicit characterization of the stability region and is used for the purpose of illustration. Other controller designs such as the hybrid predictive controller [18,30,17,32] that enable implementation of predictive controllers with a well characterized stability region can also be used to achieve fault-tolerant control within the proposed framework.

Remark 2. Note that in practical implementation when the state trajectory gets close to the desired equilibrium point, the first $(|L_{\bar{g}_k} V_k|)^2$ term in the denominator of the control law of Eq. (3.7) could cause chattering in the control action. To alleviate this chattering, a small positive number v_k may be added to the first $(|L_{\bar{g}_k} V_k|)^2$ term in the denominator. The addition of v_k allows for achieving practical stability, with decrease in magnitude of v_k (while keeping it large enough to avoid chattering) resulting in the state trajectory going further closer to the desired equilibrium point.

3.3. Fault-detection filter design

The next step in implementing fault-tolerant control is that of designing appropriate fault-detection filters that

can detect the occurrence of a fault in the control actuator by observing the behavior of the closed-loop process. To this end, we design for a given control configuration, a fault detection filter of the form:

$$\begin{aligned} \dot{w}(t) &= f_k(w(t)) + g_k(w(t))u_k(w) \\ |u_k| &\leqslant u_k^{\max} \\ r_k(t) &= \|x(t) - w(t)\| \end{aligned} \tag{3.9}$$

where $x(t) \in \mathbb{R}^7$ denotes the vector of process state variables and $u_k(t) \in [-u_k^{\max}, u_k^{\max}] \subset \mathbb{R}$ denotes the constrained manipulated input associated with the kth control configuration, $w(t) \in \mathbb{R}^7$ is the vector of filter states and $r_k(t) \in \mathbb{R}$ is the residual that detects the occurrence of a fault. The filter states are initialized at the same value as the process states ($w(0) = x(0)$) and essentially predict the evolution of the process in the absence of actuator faults. The residuals captures the difference between the predicted evolution of the states in the absence of faults and that of the process state, thereby detecting faults in the control actuators. Specifically, the value of $r_k(t)$ becomes non-zero at the earliest time that a fault occurs (for a detailed analysis of the detection properties of the filter, see [34]).

Remark 3. Note that in the presence of measurement noise, the value of $r(t)$ will be nonzero even in the absence of faults. To handle this problem, the filter should declare a fault only if the value of $r(t)$ increases beyond some threshold, δ, where δ accounts for the deviation of the plant measurements from the nominal measurements in the absence of faults (see the simulation section for a demonstration). Note also, that plant model mismatch or unknown disturbances can also cause the value of $r(t)$ to be nonzero even in the absence of faults. The FDFTC problem in the presence of time varying disturbances with known bounds on the disturbances can be handled by redesigning the filter as well as the controllers for the individual control configuration. Specifically, as in the case of measurement noise, the filter should declare a fault only if the value of $r(t)$ increases beyond some threshold, δ, where δ accounts for the deviation of the plant dynamics from the nominal dynamics in the absence of faults. The controllers for the individual control configurations need to be redesigned to mitigate the effect of disturbances on the process, in a way that allows the characterization of the robust stability regions. The robust stability region can subsequently be used in deciding which backup control configuration should be implemented in the closed-loop. With regard to the fault-detection filter, the detection threshold provides a suitable handle that can be used to achieve early fault detection. In the presence of noise, however, having a small fault-detection threshold can lead to the triggering of false alarms (as demonstrated in the simulation example) and should be picked to achieve the desired tradeoff between avoiding false alarms and detecting faults.

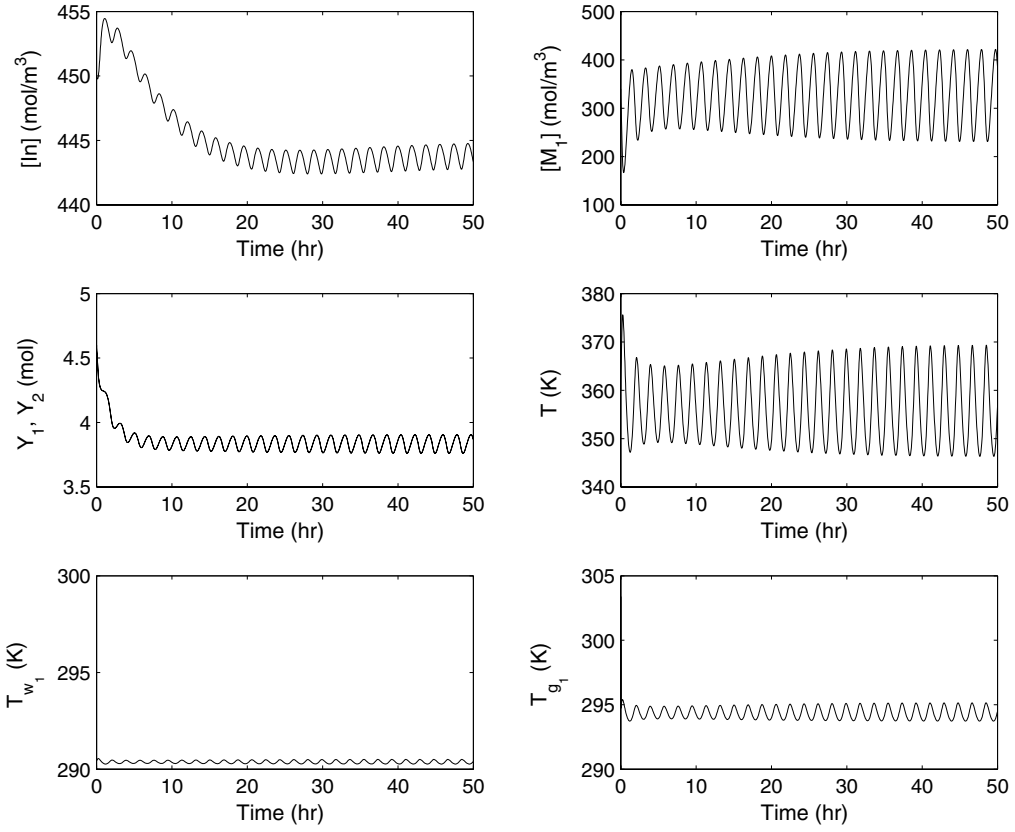

Fig. 2. Evolution of the open-loop process states.

3.4. Fault-tolerant switching logic

Having designed the feedback control laws, characterized the stability region associated with each control configuration, and designed the fault-detection filter, the fourth step is to derive the switching policy that the supervisor needs to employ to activate/deactivate the appropriate control configurations in the event of faults. The key idea here is that, because of the limitations imposed by constraints on the stability region of each configuration, the supervisor can only activate the control configuration for which the closed-loop state is within the stability region at the time of control system fault. Without loss of generality, let the initial actuator configuration be $k(0) = 1$, T_{fault} be the time when this configuration fails and let T_{detect} be the earliest time at which the value of $r_1(t) > \delta_{r_1} > 0$ (where δ_{r_1} is the detection threshold chosen based on the acceptable level of deviation of the actual closed-loop performance from the desired one), then the switching rule given by

$$k(t \geqslant T_{\text{detect}}) = 2 \quad \text{if } x(T_{\text{detect}}) \in \Omega_{c_2}(u_2^{\max}) \tag{3.10}$$

guarantees asymptotic closed-loop stability. The implementation of the above switching law requires monitoring the closed-loop state trajectory with respect to the stability regions associated with the various actuator configurations. This idea of tying the switching logic to the stability regions was first proposed in [15] for the control of switched nonlinear systems.

4. Simulation results

Several simulation runs were carried out to evaluate the effectiveness of the proposed fault-detection and fault-tolerant control strategy. Fig. 2 shows the evolution of the open-loop state profiles. Under the operating conditions listed in Table 2, the open-loop system behaves in an oscillatory fashion (i.e., the system possesses an open-loop unstable steady-state surrounded by a stable limit cycle).

First, process operation under primary control configuration was considered (i.e., the feed temperature, T_{feed}, was the manipulated input) and a bounded nonlinear controller was designed using the formula of Eqs. (3.6) and (3.7).

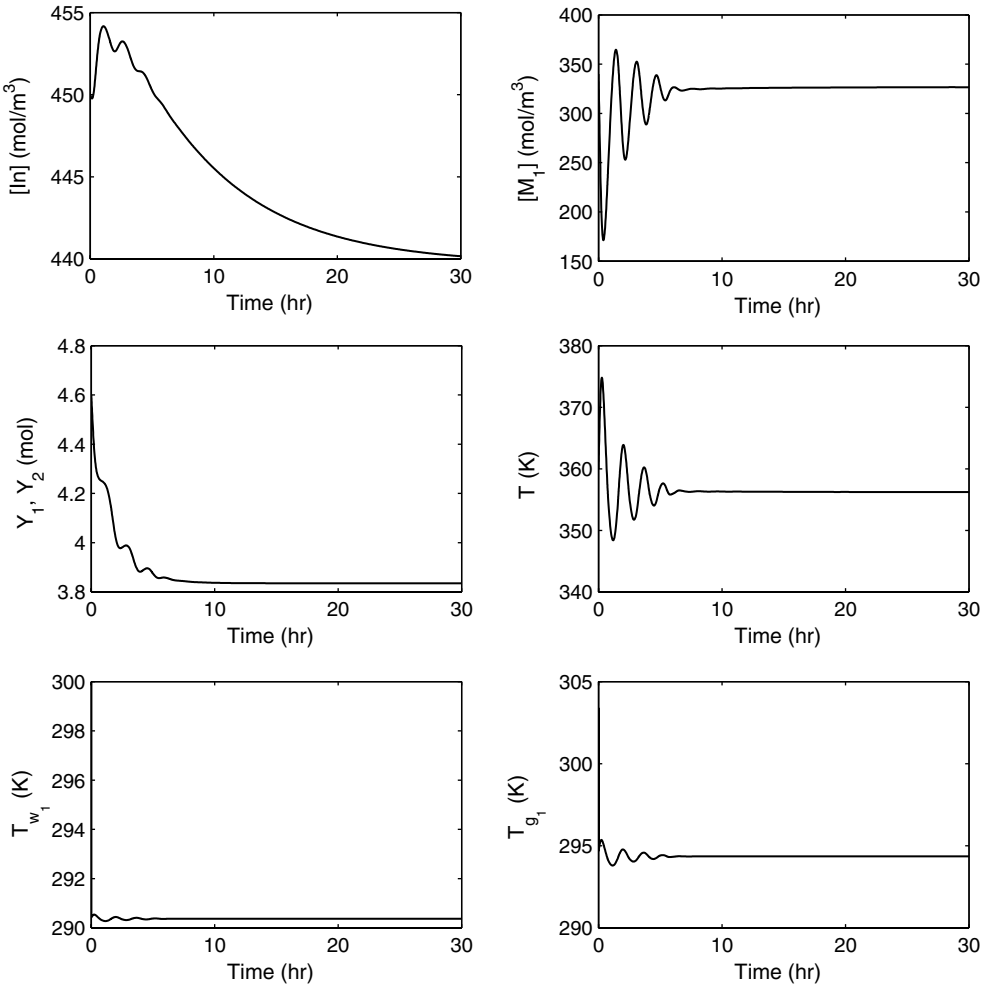

Fig. 3. Closed-loop state profiles under the primary control configuration.

Specifically, a quadratic function of the form $V_1 = \frac{1}{2}(T - T_s)^2$ and $\rho_1 = 0.01$ were used to design the controller and a composite Lyapunov function of the form $V_{c_1} = 5 \times 10^{-3}(In - In_s)^4 + 5 \times 10^{-4}(M_1 - M_{1s})^2 + 5 \times 10^{-11}(Y_1 - Y_{1s})^2 + 5 \times 10^{-11}(Y_2 - Y_{2s})^2 + 5 \times 10^{-4}(T - T_s)^2 + 5 \times 10^{-2}(T_{w_1} - T_{w_{1s}})^2 + 5 \times 10^{-11}(T_{g_1} - T_{g_{1s}})^2$ was used to estimate the stability region of the primary control configuration yielding a $c_1^{\max} = 62$.

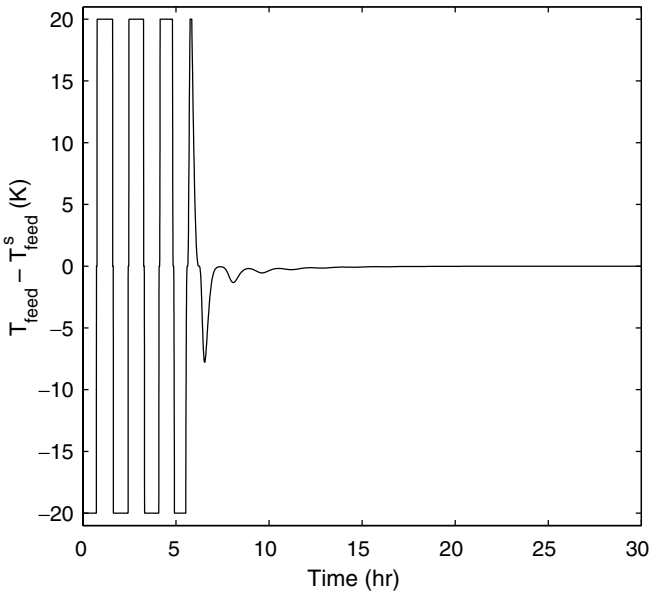

Fig. 4. Manipulated input profile under primary control configuration.

The first $(|L_{\bar{g}_k} V_k|)^2$ term in the denominator of the control law of Eq. (3.7) was replaced by $(|L_{\bar{g}_k} V_k|)^2 + v_k$ (as discussed in Remark 2), with $v_1 = 1$ and $v_2 = 5 \times 10^{-9}$, to alleviate chattering of the control action close to the desired equilibrium point under configurations 1 and 2, respectively. Fig. 3 shows the evolution of the closed-loop state profiles and Fig. 4 shows the evolution of the manipulated inputs starting from the initial condition $In(0) = 450\ \frac{\text{mol}}{\text{m}^3}$, $M_1(0) = 340\ \frac{\text{mol}}{\text{m}^3}$, $Y_1(0) = 4.6$ mol, $Y_2(0) = 4.6$ mol, $T(0) = 360$ K, $T_{w_1}(0) = 300$ K, and $T_{g_1}(0) = 300$ K for which $V_{c_1} = 61.4$. Since this initial state is within the stability region of the primary control configuration (i.e., $V_{c_1}(x(0)) \leqslant c_1^{\max}$), the primary control configuration is able to stabilize the system at the steady-state of interest.

Next, we considered the case of having a fault in the primary control configuration. In this case, the supervisor had available a fall-back control configuration with the catalyst flowrate, F_c, as the manipulated input. A quadratic Lyapunov function of the form $V_2 = e_2^{\mathrm{T}} P_2 e_2$ and $\rho_2 = 0.01$ was used to design the controller that used the fall-back control configuration and a composite Lyapunov function of the

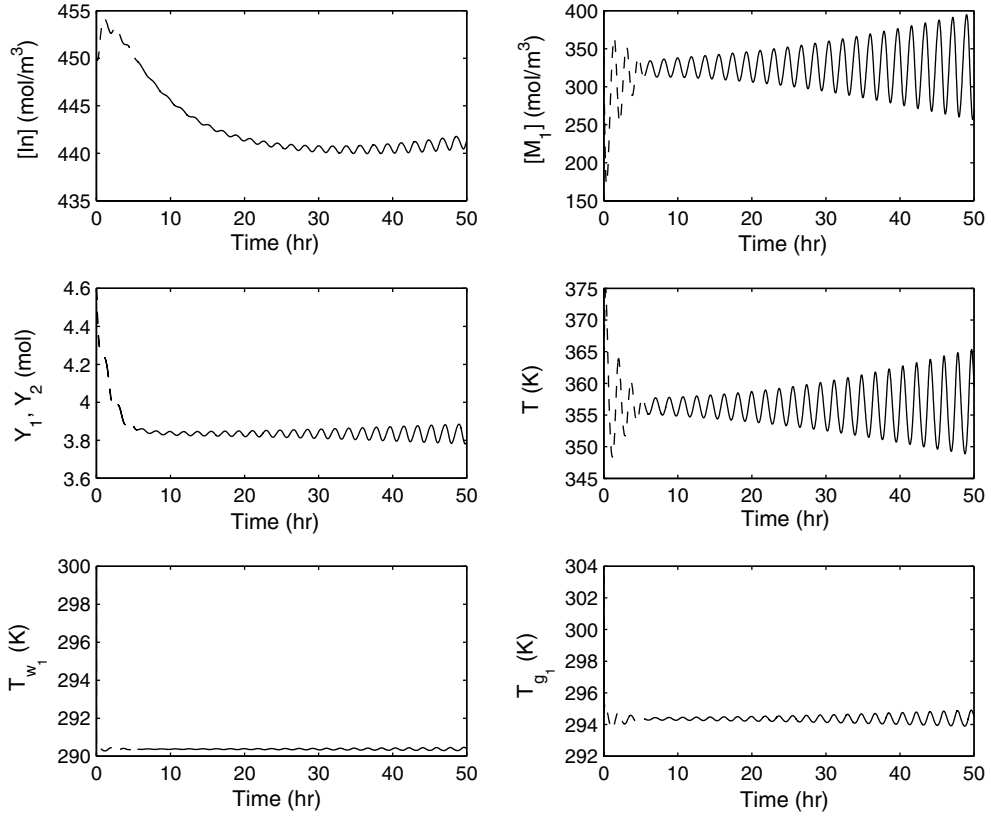

Fig. 5. Evolution of the closed-loop state profiles under primary control configuration (dashed lines) and no fall-back control configuration available to switch to (or fall-back control configuration is not activated) resulting in open-loop oscillatory behavior (solid lines) after primary control configuration fails at $T_{\text{fault}} = 5$ h 34 min.

form $V_{c_2} = 5\times10^{-3}(In - In_s)^4 + 5\times10^{-4}(M_1 - M_{1s})^2 + 5\times10^{-11}(Y_1 - Y_{1s})^2 + 5\times10^{-11}(Y_2 - Y_{2s})^2 + 5\times10^{-4}(T - T_s)^2 + 5\times10^{-11}(T_{w_1} - T_{w_{1s}})^2 + 5\times10^{-11}(T_{g_1} - T_{g_{1s}})^2$ was used to estimate the stability region of the fall-back control configuration yielding a $c_2^{\max} = 56.8$.

To demonstrate that control loop reconfiguration results in fault-tolerant reactor control in the presence of input constraints, we carried out the following simulations: We first initialized the reactor at $In(0) = 450\ \frac{\text{mol}}{\text{m}^3}$, $M_1(0) = 340\ \frac{\text{mol}}{\text{m}^3}$, $Y_1(0) = 4.6$ mol, $Y_2(0) = 4.6$ mol, $T(0) = 360$ K, $T_{w_1}(0) = 300$ K, and $T_{g_1}(0) = 300$ K resulting in $V_{c_1} = 61.4$ which implied that this initial state was within the stability region of the primary control configuration. Consider now, a fault in the primary control configuration at time $T_{\text{fault}} = 5$ h 34 min (see dashed lines in Figs. 5 and 6). In the case of no switching to fall-back control configuration or no backup control configurations available, closed-loop stability is not achieved and the process behaves in an oscillatory fashion (solid line in Fig. 5).

However, applying our fault-detection and fault-tolerant control strategy, the supervisor kept track of the residual value r_1 (see dashed line in Fig. 7) and observed the residual value r_1 becoming non-zero at $T_{\text{fault}} = 5$ h 34 min. At $T_{\text{detect}} = 5$ h 54 min, the residual value r_1 reached the detection threshold ($\delta_{r_1} = 0.5$) and a fault on primary control configuration was declared. The supervisor, then, checked if switching to fall-back control configuration would preserve stability. This was done by evaluating the value of the composite Lyapunov function

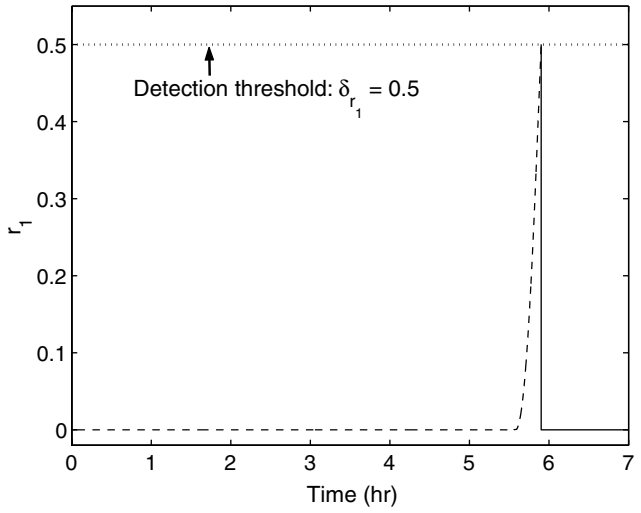

Fig. 7. Evolution of the detection filter residual value under primary control configuration (dashed line). At $T_{\text{detect}} = 5$ h 54 min, the detection filter residual value reaches the detection threshold of 0.5 which verifies that a fault on the primary control configuration occurs. A switch to the fall-back control configuration (solid line) resets the detection filter residual back to zero.

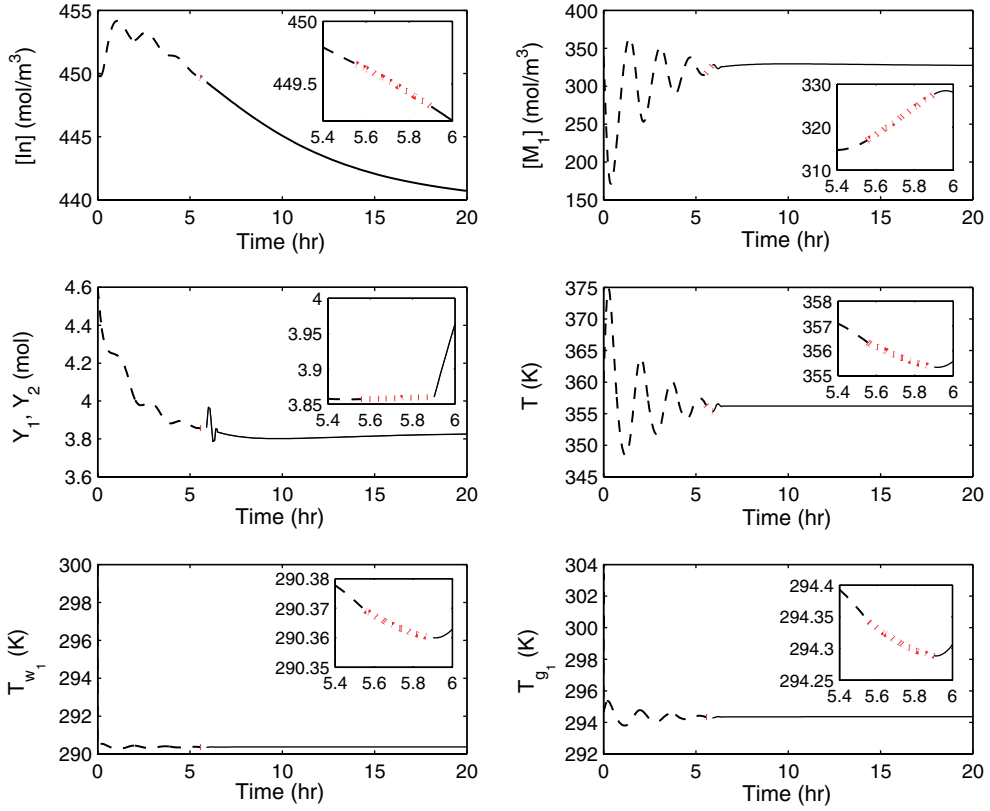

Fig. 6. Evolution of the closed-loop state profiles under primary control configuration (dashed lines) which fails at $T_{\text{fault}} = 5$ h 34 min. At this point, the process starts operating open-loop (dotted lines). At $T_{\text{detect}} = 5$ h 54 min, the detection filter verifies that there is a fault on the primary control configuration and the control system switches to the fall-back control configuration (solid lines).

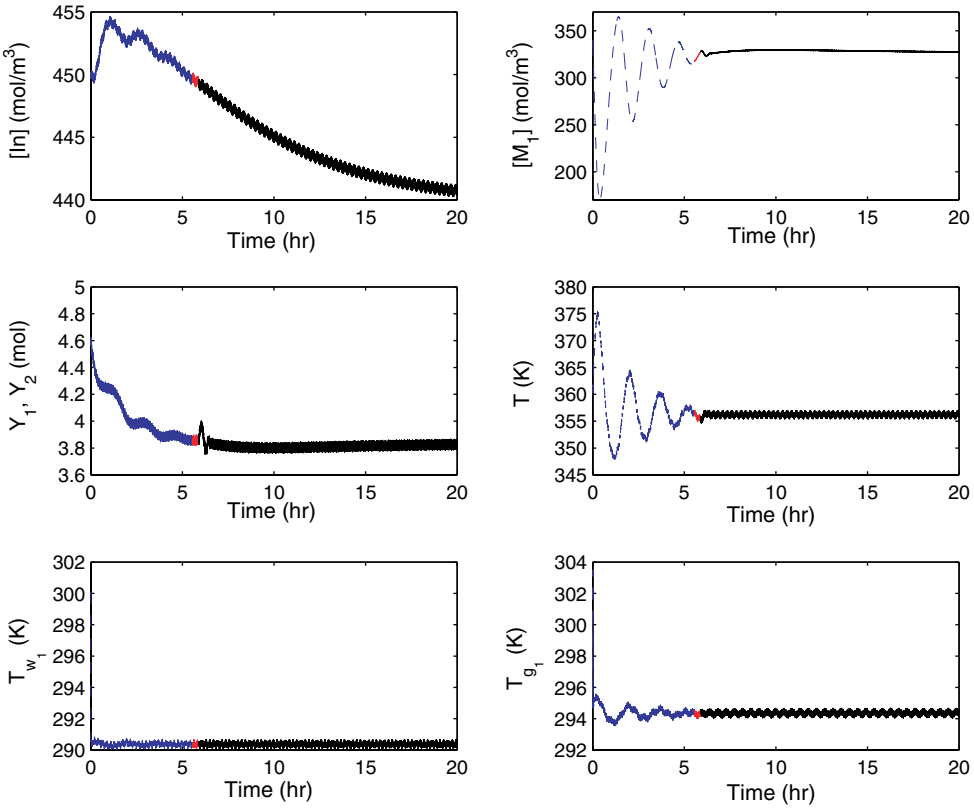

Fig. 8. Evolution of the closed-loop state profiles in the case of measurement noise under primary control configuration (dashed lines) which fails at $T_{\text{fault}} = 5$ h 34 min. At this point, the process starts operating open-loop (dotted lines). At $T_{\text{detect}} = 5$ h 54 min, the detection filter verifies that there is a fault on the primary control configuration and the control system switches to the fall-back control configuration (solid lines).

of the fall-back control configuration at $T_{\text{detect}} = 5$ h 54 min where the states were of the following values: $In(T_{\text{detect}}) = 449.7\ \frac{\text{mol}}{\text{m}^3}$, $M_1(T_{\text{detect}}) = 316.9\ \frac{\text{mol}}{\text{m}^3}$, $Y_1(T_{\text{detect}}) = 3.86$ mol, $Y_2(T_{\text{detect}}) = 3.86$ mol, $T(T_{\text{detect}}) = 356.3$ K, $T_{w_1}(T_{\text{detect}}) = 290.4$ K, and $T_{g_1}(T_{\text{detect}}) = 294.3$ K. Since $V_{c_2}(x(T_{\text{detect}})) = 49.6 \leqslant c_2^{\max}$, the state, at the time the filter detected the fault in the primary control configuration, was within the stability region of the fall-back control configuration. Therefore, switching to fall-back control configuration would preserve closed-loop stability (see solid lines in Fig. 6).

Next, we also investigated the implementation of the fault-detection and fault-tolerant control strategy in the presence of measurement noise. Specifically, we considered Gaussian measurement noise of the following magnitude: $In = 0.5\ \frac{\text{mol}}{\text{m}^3}$, $M_1 = 0.3\ \frac{\text{mol}}{\text{m}^3}$, $Y_1 = 0.04$ mol, $Y_2 = 0.04$ mol, $T = 0.8$ K, $T_{w_1} = 0.3$ K, and $T_{g_1} = 0.3$ K. Note that in the presence of measurement noise, the value of the residual stayed non-zero even in the absence of actuator faults (for the measurement noise considered in this study, a detection threshold of $\delta_{r_1} = 0.5$ was no longer appropriate and triggered false alarms). A new threshold that captured the effect of the measurement noise on the value of the residual was needed. A detection threshold of $(\delta_{r_1} = 0.7)$ was then picked. Consider once again a fault in the primary control configuration at time $T_{\text{fault}} = 5$ h 34 min. This fault was detected by the fault-detection filter via the residual reaching the threshold at $T_{\text{detect}} = 5$ h 54 min (see dashed line in Fig. 9). The supervisor, then, checked

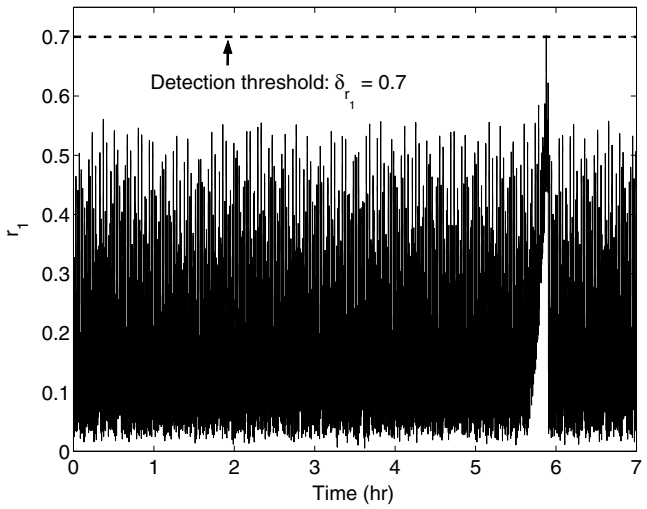

Fig. 9. Evolution of the detection filter residual value in the case of measurement noise. A detection threshold of 0.5 triggers false alarm even before real fault on primary control configuration at $T_{\text{fault}} = 5$ h 34 min. A new detection threshold of 0.7 is picked and implemented. At $T_{\text{detect}} = 5$ h 54 min, the detection filter residual value reaches the detection threshold of 0.7 which verifies that a fault on the primary control configuration occurs. A switch to the fall-back control configuration resets the detection filter residual back to normal.

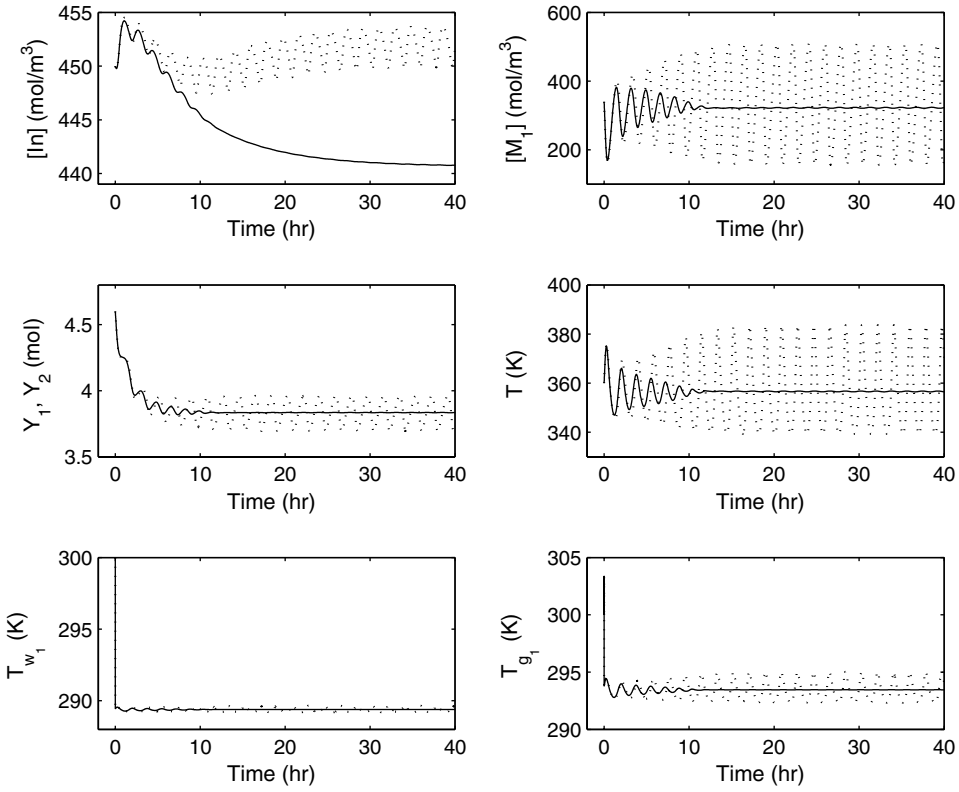

Fig. 10. Evolution of the open-loop (dotted lines) and closed-loop (solid lines) state profiles under the primary control configuration in the presence of parametric model uncertainty and disturbances.

if switching to fall-back control configuration would preserve stability. As before, this was done by evaluating the value of the composite Lyapunov function of the fall-back control configuration at $T_{\text{detect}} = 5$ h 54 min where the states were of the following values: $In(T_{\text{detect}}) = 449.3\ \frac{\text{mol}}{\text{m}^3}$, $M_1(T_{\text{detect}}) = 327.5\ \frac{\text{mol}}{\text{m}^3}$, $Y_1(T_{\text{detect}}) = 3.83$ mol, $Y_2(T_{\text{detect}}) = 3.83$ mol, $T(T_{\text{detect}}) = 355.6$ K, $T_{w_1}(T_{\text{detect}}) = 290.4$ K, and $T_{g_1}(T_{\text{detect}}) = 294.4$ K. Since $V_{c_2}(x(T_{\text{detect}})) = 42.7 \leqslant c_2^{\max}$, the state, at the time the filter detected the fault in the primary control configuration, was within the stability region of the fall-back control configuration. Subsequent switching to the fall-back control configuration once again resulted in closed-loop stability (see solid lines in Fig. 8).

Finally, we also evaluated the robustness of the controller that is a vital component of the fault-tolerant control structure. We considered values of some of the process parameters being different from the ones used in the controller design, specifically, $E_a = 38.058$ kJ/mol and $H_{\text{reac}} = 3780.429$ kJ/kg and also in the presence of disturbance in the inlet coolant temperature, with $T_{wi} = 288.56$ K. The dotted lines in Fig. 10 shows the open-loop profiles illustrating the effect of the presence of disturbances and uncertainty in the parameters on the process states. In contrast, when the primary control configuration is implemented, the controller is able to reject the disturbances and stabilize the process at the desired equilibrium point (see solid lines in Fig. 10).

5. Conclusions

In this work we focused on fault-tolerant control of a gas phase polyethylene reactor. Initially, a family of candidate control configurations, characterized by different manipulated inputs, were identified. For each control configuration, a bounded nonlinear feedback controller, that enforced asymptotic closed-loop stability in the presence of constraints, was designed, and the constrained stability region associated with it was explicitly characterized using Lyapunov-based tools. A fault-detection filter was designed to detect the occurrence of a fault in the control actuator by observing the deviation of the process states from the expected closed-loop behavior. A switching policy was then derived, on the basis of the stability regions, to orchestrate the activation/deactivation of the constituent control configurations in a way that guaranteed closed-loop stability in the event of control system faults. Closed-loop simulations were carried out to implement the fault-tolerant control strategy on the gas phase polyethylene reactor and to demonstrate the implementation of the fault-tolerant control method in the presence of measurement noise.

Acknowledgement

Financial support from NSF, CTS-0529295, is gratefully acknowledged.

References

[1] H.B. Aradhye, B.R. Bakshi, J.F. Davis, S.C. Ahalt, Clustering in wavelet domain: a multiresolution art network for anomaly detection, AIChE Journal 50 (2004) 2455–2466.

[2] J. Bao, W.Z. Zhang, P.L. Lee, Passivity-based decentralized failure-tolerant control, Industrial & Engineering Chemistry Research 41 (2002) 5702–5715.

[3] M. Blanke, R. Izadi-Zamanabadi, S.A. Bogh, C.P. Lunau, Fault-tolerant control systems – a holistic view, Control Engineering Practice 5 (1997) 693–702.

[4] K.-Y. Choi, W.H. Ray, The dynamic behavior of fluidized-bed reactors for solid catalyzed gas-phase olefin polymerization, Chemical Engineering Science 40 (1985) 2261–2279.

[5] P.D. Christofides, N.H. El-Farra, Control of Nonlinear and Hybrid Process Systems: Designs for Uncertainty, Constraints and Time-Delays, Springer, New York, 2005.

[6] S.A. Dadebo, M.L. Bell, P.J. McLellan, K.B. McAuley, Temperature control of industrial gas phase polyethylene reactors, Journal of Process Control 7 (1997) 83–95.

[7] J.F. Davis, M.L. Piovoso, K. Kosanovich, B. Bakshi, Process data analysis and interpretation, Advances in Chemical Engineering 25 (1999) 1–103.

[8] R.A. Decarlo, M.S. Branicky, S. Petterson, B. Lennartson, Perspectives and results on the stability and stabilizability of hybrid systems, Proceedings of the IEEE 88 (2000) 1069–1082.

[9] M.A. Demetriou, A model-based fault detection and diagnosis scheme for distributed parameter systems: a learning systems approach, ESAIM-Control Optimisation and Calculus of Variations 7 (2002) 43–67.

[10] C. DePersis, A. Isidori, A geometric approach to nonlinear fault detection and isolation, IEEE Transactions on Automatic Control 46 (2001) 853–865.

[11] R. Dunia, S.J. Qin, Subspace approach to multidimensional fault identification and reconstruction, AIChE Journal 44 (1998) 1813–1831.

[12] R. Dunia, S.J. Qin, T.F. Edgar, T.J. McAvoy, Identification of faulty sensors using principal component analysis, AIChE Journal 42 (1996) 2797–2812.

[13] N.H. El-Farra, P.D. Christofides, Integrating robustness, optimality, and constraints in control of nonlinear processes, Chemical Engineering Science 56 (2001) 1841–1868.

[14] N.H. El-Farra, P.D. Christofides, Bounded robust control of constrained multivariabe nonlinear processes, Chemical Engineering Science 58 (2003) 3025–3047.

[15] N.H. El-Farra, P.D. Christofides, Coordinated feedback and switching for control of hybrid nonlinear processes, AIChE Journal 49 (2003) 2079–2098.

[16] N.H. El-Farra, A. Gani, P.D. Christofides, Fault-tolerant control of process systems using communication networks, AIChE Journal 51 (2005) 1665–1682.

[17] N.H. El-Farra, P. Mhaskar, P.D. Christofides, Hybrid predictive control of nonlinear systems: method and applications to chemical processes, International Journal of Robust and Nonlinear Control 4 (2004) 199–225.

[18] N.H. El-Farra, P. Mhaskar, P.D. Christofides, Uniting bounded control and MPC for stabilization of constrained linear systems, Automatica 40 (2004) 101–110.

[19] P.M. Frank, Fault diagnosis in dynamic systems using analytical and knowledge-based redundancy – a survey and some new results, Automatica 26 (1990) 459–474.

[20] P.M. Frank, X. Ding, Survey of robust residual generation and evaluation methods in observer-based fault detection systems, Journal of Process Control 7 (1997) 403–424.

[21] V. Garcia-Onorio, B.E. Ydstie, Distributed, asynchronous and hybrid simulation of process networks using recording controllers, International Journal of Robust and Nonlinear Control 14 (2004) 227–248.

[22] I.E. Grossmann, S.A. van den Heever, I. Harjukoski, Discrete optimization methods and their role in the integration of planning and scheduling, in: Proceedings of 6th International Conference on Chemical Process Control, Tucson, AZ, 2001, pp. 124–152.

[23] K.M. Hangos, J.B. Varga, F. Friedler, L.T. Fan, Integrated synthesis of a process and its fault-tolerant control-system, Computers and Chemical Engineering 19 (1995) S465–S470.

[24] I. Hyanek, J. Zacca, F. Teymour, W.H. Ray, Dynamics and stability of polymerization process flow sheets, Industrial & Engineering Chemistry Research 34 (1995) 3872–3877.

[25] J.V. Kresta, J.F. Macgregor, T.E. Marlin, Multivariate statistical monitoring of process operating performance, Canadian Journal of Chemical Engineering 69 (1991) 35–47.

[26] Y. Lin, E.D. Sontag, A universal formula for stabilization with bounded controls, Systems & Control Letters 16 (1991) 393–397.

[27] M. Massoumnia, G.C. Verghese, A.S. Wilsky, Failure detection and identification, IEEE Transactions on Automatic Control 34 (1989) 316–321.

[28] K.B. McAuley, D.A. Macdonald, P.J. McLellan, Effects of operating conditions on stability of gas-phase polyethylene reactors, AIChE Journal 41 (1995) 868–879.

[29] N. Mehranbod, M. Soroush, C. Panjapornpon, A method of sensor fault detection and identification, Journal of Process Control 15 (2005) 321–339.

[30] P. Mhaskar, N.H. El-Farra, P.D. Christofides, Hybrid predictive control of process systems, AIChE Journal 50 (2004) 1242–1259.

[31] P. Mhaskar, N.H. El-Farra, P.D. Christofides, Predictive control of switched nonlinear systems with scheduled mode transitions, IEEE Transactions on Automatic Control 50 (2005) 1670–1680.

[32] P. Mhaskar, N.H. El-Farra, P.D. Christofides, Robust hybrid predictive control of nonlinear systems, Automatica 41 (2005) 209–217.

[33] P. Mhaskar, A. Gani, P.D. Christofides, Fault-tolerant control of nonlinear processes: performance-based reconfiguration and robustness, International Journal of Robust and Nonlinear Control 16 (2006) 91–111.

[34] P. Mhaskar, A. Gani, C. McFall, N.H. El-Farra, P.D. Christofides, J.F. Davis, Integrated fault-detection and fault-tolerant control for process systems, AIChE Journal 52 (2006) 2129–2148.

[35] A. Negiz, A. Cinar, Statistical monitoring of multivariable dynamic processes with state-space models, AIChE Journal 43 (1997) 2002–2020.

[36] P. Nomikos, J.F. Macgregor, Monitoring batch processes using multiway principal component analysis, AIChE Journal 40 (1994) 1361–1375.

[37] R.J. Patton, Fault-tolerant control systems: the 1997 situation, in: Proceedings of the IFAC Symposium, SAFEPROCESS 1997, Hull United Kingdom, 1997, pp. 1033–1054.

[38] J. Prakash, S.C. Patwardhan, S. Narasimhan, A supervisory approach to fault-tolerant control of linear multivariable systems, Industrial & Engineering Chemistry Research 41 (2002) 2270–2281.

[39] D.K. Rollins, J.F. Davis, Unbiased estimation technique when gross errors exist in process measurements, AIChE Journal 38 (1992) 563–572.

[40] A. Saberi, A.A. Stoorvogel, P. Sannuti, H. Niemann, Fundamental problems in fault detection and identification, International Journal of Robust and Nonlinear Control 10 (2000) 1209–1236.

[41] D.D. Siljak, Reliable control using multiple control systems, International Journal of Control 31 (1980) 303–329.

[42] E. Tatara, A. Cinar, An intelligent system for multivariate statistical process monitoring and diagnosis, ISA Transactions 41 (2002) 255–270.

[43] N.E. Wu, K.M. Zhou, G. Salomon, Control reconfigurability of linear time-invariant systems, Automatica 36 (2000) 1767–1771.

[44] T.Y. Xie, K.B. McAuley, J.C.C. Hsu, D.W. Bacon, Gas-phase ethylene polymerization – production processes, polymer properties, and reactor modeling, Industrial & Engineering Chemistry Research 33 (1994) 449–479.

[45] G.H. Yang, S.Y. Zhang, J. Lam, J. Wang, Reliable control using redundant controllers, IEEE Transactions on Automatic Control 43 (1998) 1588–1593.

[46] X.D. Zhang, T. Parisini, M.M. Polycarpou, Adaptive fault-tolerant control of nonlinear uncertain systems: an information-based diagnostic approach, IEEE Transactions on Automatic Control 49 (2004) 1259–1274.

[47] D.H. Zhou, P.M. Frank, Fault diagnostics and fault tolerant control, IEEE Transactions on Aerospace and Electronic Systems 34 (1998) 420–427.